

# Transverse Beam Characterization in the CEBAF 5 MeV Region

*C. Tennant, J. Grames, R. Suleiman, D. Turner*

## Abstract

In this note we report the results of quadrupole scan measurements in the 5 MeV region of CEBAF. Using quadrupole 0L02 and the harp at 0L03 we simultaneously scanned both transverse planes. Beam sizes were extracted using several methods - the most robust using an asymmetric Gaussian fit. Beam Twiss parameters and emittances were calculated which, in turn, allowed us to estimate the beam parameters at the entrance to the quarter cryounit (500 keV region).

## Introduction

Having a good understanding of the beam dynamics in the 5 MeV region – from the exit of the capture to the entrance of cryomodule 0L03 – is vitally important. The cryounit marks the hand off of the low energy beamline, owned and modeled by the injector group using space charge codes to the relativistic, *elegant*-driven [1] modeling done in CASA. Additionally, the 5D line in this region successfully supported the Polarized Electrons for Polarized Positrons (PEPPo) experiment [2] and will support a Bubble Chamber experiment [3] in the near future; both of which require knowledge of the beam properties.

## Measurement

A schematic of a portion of the 5 MeV region is depicted in Figure 1. With a harp at 0L03 it remains to find what upstream quadrupole is best suited for scanning. The quadrupoles at 0L03 and 0L03A are too close to the harp. Using the quadrupole at 0L02, with downstream quadrupoles turned off, was simulated to have the best performance. In the end this amounts to a simple quad-drift scan with a drift length of 6.629806 m from the exit of 0L02 to the harp (IHA0L03). Furthermore, both planes can be scanned simultaneously and the beam size is large enough so that wire thickness (25  $\mu\text{m}$ ) has a negligible effect [4].

Opportunistic measurements were made on February 19, 2014 before the start of Mott studies. Consequently the beam momentum was 5.487 MeV/c rather than the standard 6.3 MeV/c. The quadrupole was scanned from 5.5 to  $-3.5 \text{ m}^{-2}$  in steps of  $1 \text{ m}^{-2}$ .

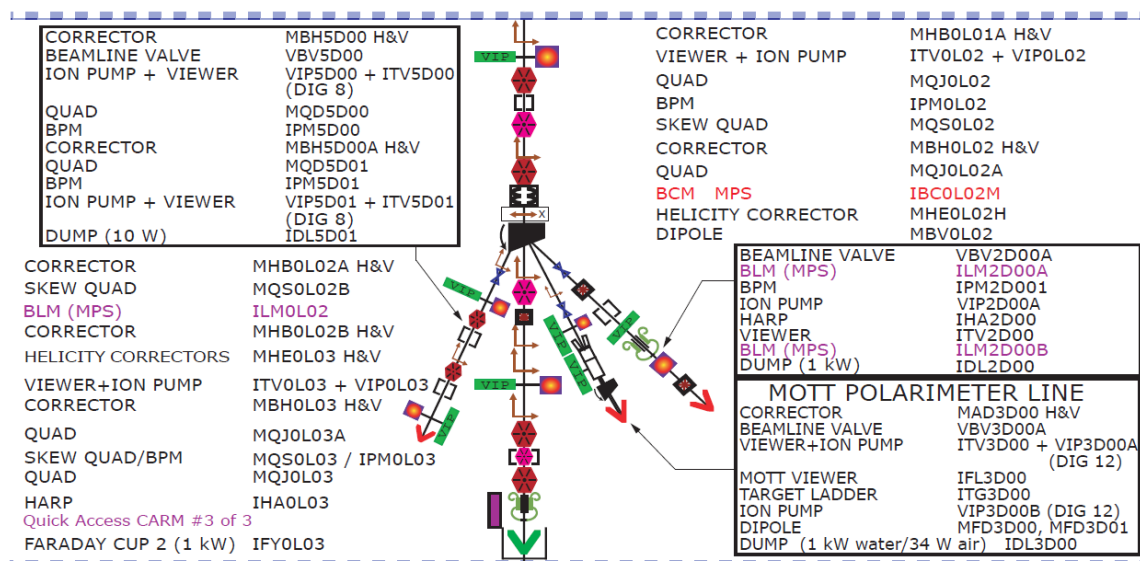


Figure 1: Schematic of the 5 MeV region showing the location of the scanning quadrupole (MQJ0L02) and harp (IHA0L03).

## Extracting Beam Sizes

We computed beam sizes using three different methods; the Harp Analyzer tool, using a Gaussian distribution to fit the profiles and using an asymmetric Gaussian distribution for the fits. Each is described briefly.

### Harp Analyzer Tool

When the three profiles (for a 3-wire harp) are well separated and Gaussian, the Harp Analyzer tool does a good job of fitting and computing the beam size. There are, however, instances when it inexplicably does not fit them (see Fig. 2). Consequently, we did a more careful analysis off-line.

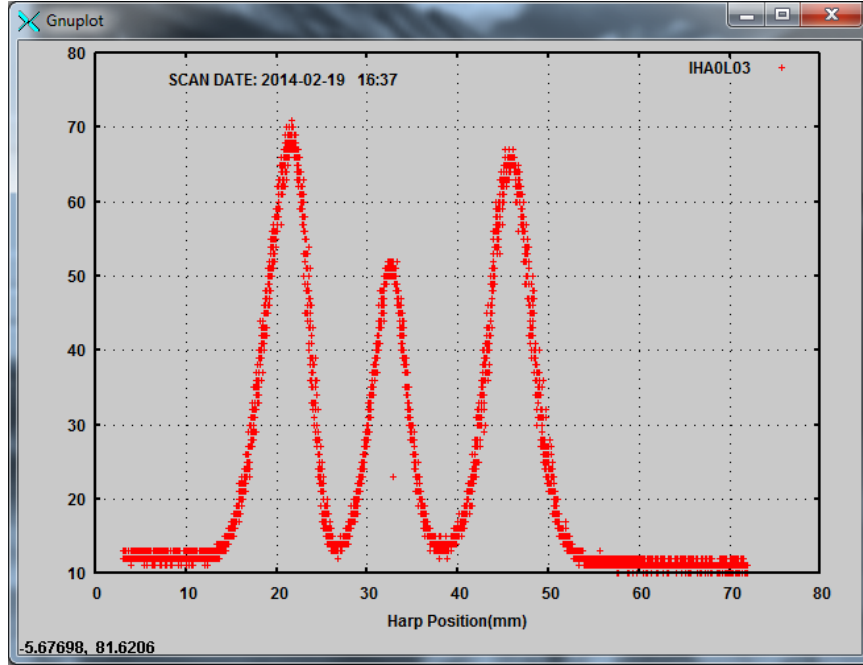


Figure 2: Screen shot from Harp Analyzer showing an example scan for which fits were not computed: “ERROR: Did not find enough peaks, IHA0L03 has 3 wires”.

### Gaussian

Due to the close proximity of the peaks during some of the scans, fits were constrained to user-defined regions. This allowed us to fit peaks which the Harp Analyzer could not.

### Asymmetric Gaussian

During an emittance measurement when the Harp Analyzer tool displays the fits to the peaks (assuming it can fit them), they generally look quite good. However, when analyzing the data off-line it was quite evident that the horizontal profile, in particular, was an asymmetric Gaussian. To better fit the data we followed the procedure in Ref. [5]. That is, rather than a Gaussian fit of the form

$$A + B \cdot g(x - x_o) \quad (1)$$

where

$$g(x) = \frac{1}{\sqrt{2\pi}\sigma} \exp\left(\frac{-x^2}{2\sigma^2}\right) \quad (2)$$

we include an additional fitting parameter,  $E$ ,

$$g(x) = \frac{1}{\sqrt{2\pi}\sigma} \exp\left(\frac{-x^2}{2(\sigma(1+\text{sign}(x) \cdot E))^2}\right) \quad (3)$$

From the fit it is straightforward to compute the rms width as

$$rms = \sigma \cdot \sqrt{1 + \left(3 - \frac{8}{\pi}\right) \cdot E^2} \quad (4)$$

An example of how an asymmetric compares to a normal (symmetric) Gaussian is shown in Fig. 3. If profiles do exhibit asymmetry, using a Gaussian fit will consistently underestimate the beam size. (A complete list of the extracted beam sizes is given in Appendix A).

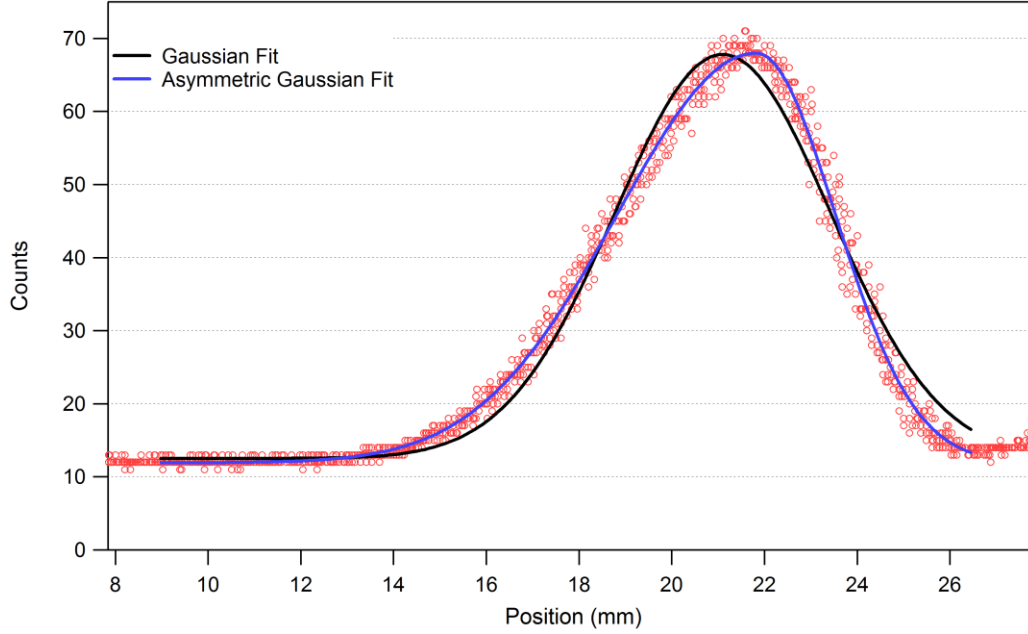


Figure 3: Example of a measured horizontal beam profile with Gaussian (black) and asymmetric Gaussian (blue) fits.

## Analysis and Results

With beam sizes extracted, we started fitting the data to compute Twiss parameters and emittances. The analysis was performed with a custom program written in Igor Pro (initially to analyze harp scans from the CEBAF-ER experiment [6]), a FORTRAN program used in the early days of CEBAF [7] and the *sddsemitproc* routine available in the SDDS Tool Kit [8]. Note, that the first two are based on a multiple regression fit (and give the exact same answers), while the *sddsemitproc* routine utilizes a robust least squares fit.

Figure 4 shows the beam size squared versus the magnification (or,  $M_{11}$  matrix element) for the horizontal and vertical scans and fits. Ideally several more vertical scans would be taken to improve the fitting; however due to time constraints – and the fact that a single stroke/measurement requires 2 minutes – we were unable to.

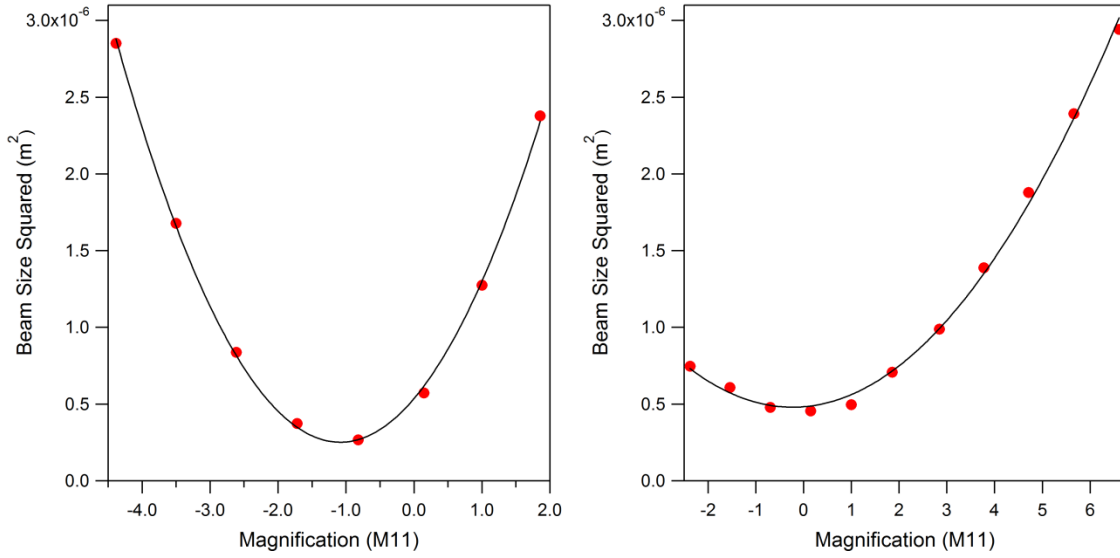


Figure 4: Horizontal (left) and vertical (right) scans with fit.

The result of using a multiple regression fit on the three sets of beam size data are given in Table 1. As a reminder, these values correspond to the entrance of the scanning quadrupole (MQJ0L02). Table 2 gives the values computed by the *sddsemitproc* routine using the beam sizes from asymmetric Gaussian fits only.

Table 1: Analysis results of multiple regression fits of three sets of beam size data.

	<b>Harp Analyzer</b>	<b>Gaussian</b>	<b>Asymmetric Gaussian</b>
$\epsilon_x$ (mm-mrad)	0.3777	0.3858	0.3958
$\epsilon_y$ (mm-mrad)	0.2566	0.2571	0.2576
$\beta_x$ (m)	5.3536	6.3612	6.3709
$\beta_y$ (m)	2.0776	2.2375	2.2333
$\alpha_x$	-0.8341	-1.0632	-1.0370
$\alpha_y$	-0.0419	-0.0427	-0.0458

Table 2: Analysis results of *sddsemitproc* fits of beam size data.

	<b>Asymmetric Gaussian</b>
$\epsilon_x$ (mm-mrad)	0.3933
$\epsilon_y$ (mm-mrad)	0.2594
$\beta_x$ (m)	6.3812
$\beta_y$ (m)	2.3417
$\alpha_x$	-1.0169
$\alpha_y$	-0.0182

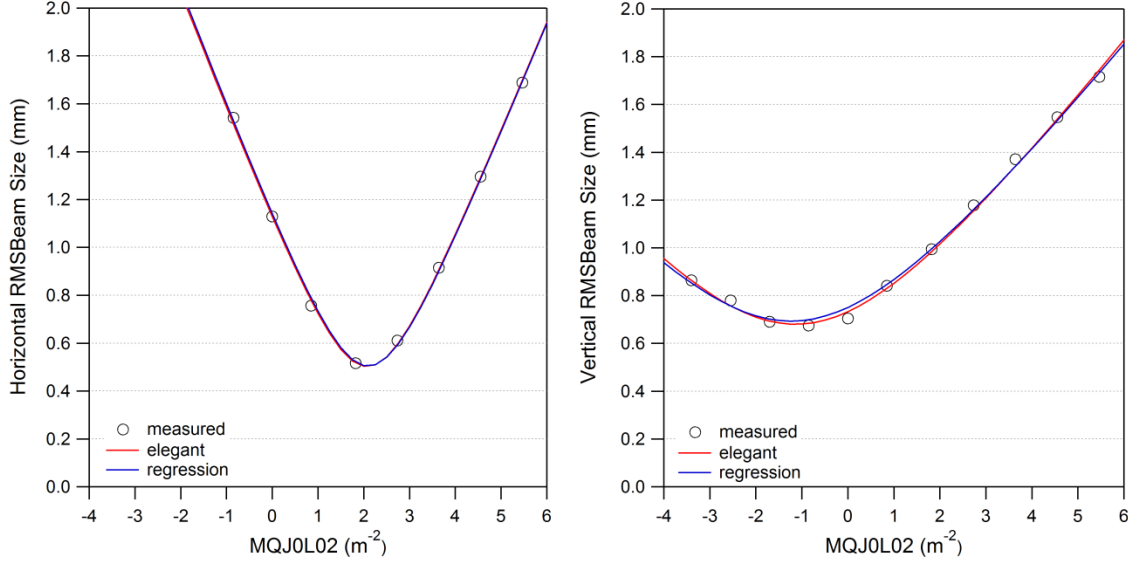


Figure 5: Simulated horizontal (left) and vertical (right) scans using extracted Twiss parameters.

As a test, we simulated the quadrupole scan using the results from fitting with asymmetric Gaussians and compared the regression and least squares fit. The *sddsemitproc* results (labeled as “elegant” in the legend) show a better fit to the vertical data, particularly near the minimum. This difference is reflected in the discrepancy in the vertical betas and alphas (compare Tables 1 and 2 for the “Asymmetric Gaussian”). Whereas the emittance and horizontal Twiss parameters exhibit discrepancies on the order of 1%, the vertical beta and alpha differ by 5% and a factor of 2.5, respectively. Much of this could be resolved by having a larger set of data points to fit.

A helpful way to visualize the measured parameters of a quadrupole scan ( $\beta$ ,  $\alpha$ ,  $\varepsilon$ ) is to generate the associated phase ellipse. Figure 6 shows a comparison of the transverse phase ellipses at the entrance to quadrupole 0L02 from measurements and from design values. We note that the origin of the design  $\beta$  and  $\alpha$  values (as found in the elegant decks) are cloaked in mystery and so disagreement with them is neither unexpected nor particularly troubling. We note further that the elegant deck describes the beam with a normalized emittance of 1 mm-mrad – much too large even under pessimistic assumptions. Absent recent measurements, a value of 0.13 mm-mrad was assumed for each transverse plane [9].

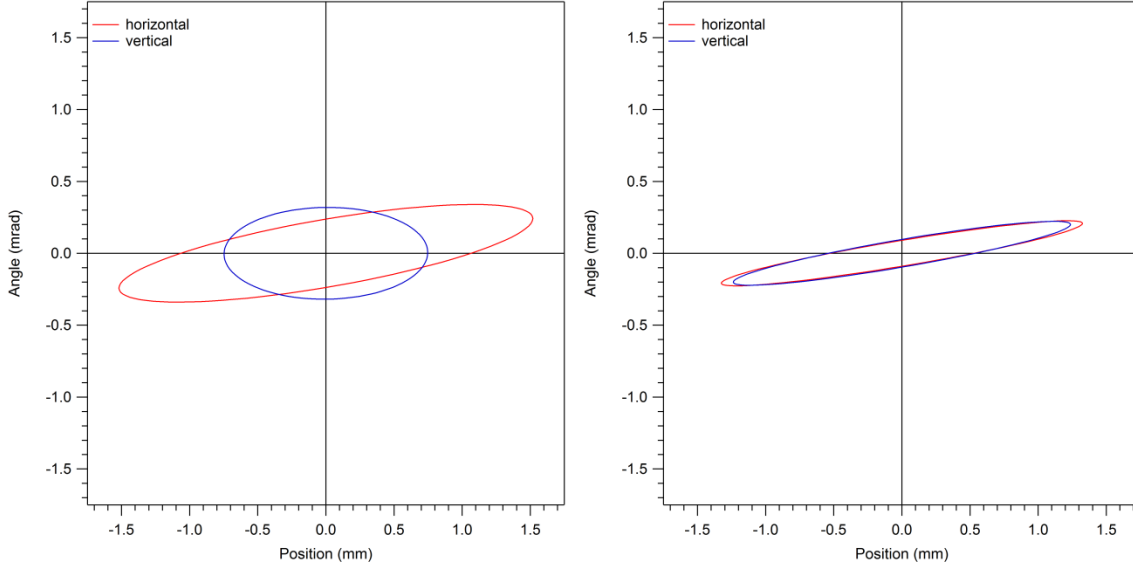


Figure 6: Transverse phase ellipses at the entrance to MQJ0L02 from measurements (left) and from design values (right).

## Back Propagation to the Entrance of the Quarter Cryounit

Because these measurements were not taken at the standard 6.3 MeV/c, it will be difficult to compare future measurements. Moving to a different energy setpoint requires changing the gradients in the quarter cryounit; this in turn changes the RF transverse focusing which the nonrelativistic beam is particularly sensitive to. An effort was made to back propagate these results to a location upstream of where changes were made, i.e. the cryounit. This was done by creating a model of the beamline from the entrance to the cryounit to the entrance of quadrupole 0L02 in Parmela [10]. Though typically reserved for space charge calculations, Parmela has the capability to read in cavity field profiles and perform detailed beam dynamics calculations; including time-of-flight effects for sub-relativistic particles. By propagating principle rays through the beamline, one can compute the transfer matrix for the system. Knowing this matrix and the measured Twiss values, it is straightforward to back out what the initial Twiss parameters must be (see Table 3). The associated phase space ellipses are shown in Fig. 7.

Table 3:

Parameter	Cryounit Entrance
$\epsilon_{x,y}$ (mm-mrad)	0.3933, 0.2594
$\beta_{x,y}$ (m)	1.3892, 4.0910
$\alpha_{x,y}$	-0.7894, -2.9916

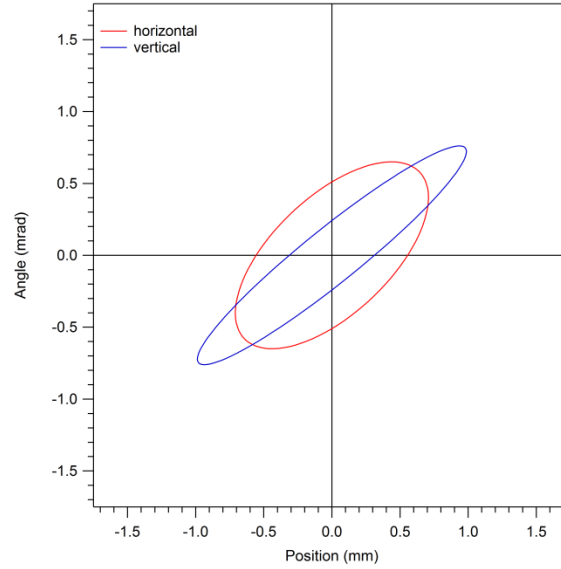


Figure 7: Estimates of the transverse phase ellipses at the entrance to the quarter cryounit (540 keV).

We caution that this is only an estimate and that this calculation has many assumptions. Namely,

- The kinetic energy at the exit of the capture section has not been measured, though a plan is in place [11]. For this work, a value of 540 keV was used.
- A rough model of the cryounit was used (i.e. details of inter-cavity spacing, distances to flanges are probably close, but not exact).
- A thorough analysis requires a 3D model of the cavities. It is well known that trapped fields in cavity end groups can cause focusing (quadrupole and skew quadrupole) and steering (dipole) effects [12]. Years ago there was a study of the FEL injector using a 3D Parmela model [13]. However the principle owners of that deck have since left the laboratory.
- It's assumed that the emittance remains constant. Given the low energy of the beam and the aforementioned trapped fields, this is highly unlikely.
- This did not include the effects from space charge (though a single run with 20 fC showed negligible effect on the results).

## Summary

Beam Twiss parameters and emittance in both transverse planes have been measured at 5.487 MeV/c. Improved fitting of beam profiles was shown by using an asymmetric Gaussian. No attempt of error analysis has been made at this stage (we leave that as an exercise for the reader). Additionally, using the measurements as a starting point, we made estimates of the beam properties at the entrance of the cryounit. More accurate results require further effort to model the 3D cavity effects.



## References

- [1] M. Borland, “*elegant: A Flexible SDDS-Compliant Code for Accelerator Simulation*”, Advanced Photon Source LS-287 (2000).
- [2] J. Grames, “*PEPPo: Using a Polarized Electron Beam to Produce PPolarized Positrons*”, Proceedings of the 2013 Workshop on Polarized Sources, Targets and Polarimetry (2013). (see <http://tinyurl.com/ntwb2n4>)
- [3] C. Ugalde et al., “*Measurement of  $^{16}\text{O}(\gamma,\alpha)^{12}\text{C}$  with a Bubble Chamber and a Bremsstrahlung Beam*”, PAC proposal (2013). (see <http://tinyurl.com/nsph5ce>)
- [4] A. Freyberger, “*Wire Scanner Response*”, Jefferson Lab Tech Note 14-002 (2014).
- [5] F.-J. Decker, “*Beam Distributions Beyond RMS*”, SLAC-PUB-6684 (1994).
- [6] C. Tennant, “*Analysis of Emittance Measurements of the Energy-Recovered Beam in CEBAF-ER*”, Jefferson Lab Tech Note 03-044 (2003).
- [7] Courtesy D. Douglas
- [8] <http://tinyurl.com/lzhdken>
- [9] see ELOG #3264002 (<https://logbooks.jlab.org/entry/3264002>)
- [10] L. Young, “*Parmela Documentation*”, LANL LA-UR-96-1835 (2005).
- [11] Y. Wang, *private communication* (2014).
- [12] Z. Li, “*Beam Dynamics in the CEBAF Superconducting Cavities*”, Ph.D. Thesis, The College of William & Mary (1995).
- [13] D. Douglas and C. Hernandez-Garcia, *private communication* (2014).

## Appendix A: Beam Size Data

For completeness a table of the extracted beam sizes is given below. The red entries denote computed rms values from the Harp Analyzer tool (it would not report sigma values). The last three horizontal measurements (denoted in gray) under the “Gaussian” and “Asymmetric Gaussian” columns were computed when the horizontal profile was merged with the adjacent profile (see Fig. A1). Since the horizontal scan already had sufficient data and went through a well-defined minimum, these partial fits were omitted in the analysis.

Table A1: Extracted horizontal and vertical beam sizes during a scan of MQJ0L02.

	MQJ0L02		Harp Analyzer		Gaussian		Asymmetric Gaussian	
	m <sup>-2</sup>	Gauss	x (mm)	y (mm)	x (mm)	y (mm)	x (mm)	y (mm)
IHA0L03 4:37	5.4637	150.0008	1.5707	1.6567	1.6520	1.7134	1.6884	1.7154
IHA0L03 4:39	4.5531	125.0011	1.1926	1.5056	1.2640	1.5429	1.2953	1.5468
IHA0L03 4:40	3.6425	100.0012	0.8858	1.4093	0.8964	1.3673	0.9154	1.3705
IHA0L03 4:42	2.7318	74.9988	0.6000	1.1623	0.6059	1.1766	0.6105	1.1780
IHA0L03 4:44	1.8212	49.9993	0.5095	0.9827	0.5140	0.9911	0.5166	0.9945
IHA0L03 4:45	0.8496	23.3249	0.7420	0.8222	0.7485	0.8372	0.7568	0.8412
IHA0L03 4:47	0.0000	0.0000	1.1070	0.7381	1.1225	0.7019	1.1289	0.7042
IHA0L03 4:49	-0.8496	-23.3249	1.3563	0.6938	1.5386	0.6745	1.5420	0.6751
IHA0L03 4:50	-1.6992	-46.6499	---	0.6915	2.0393	0.6930	1.3750	0.6912
IHA0L03 4:52	-2.5488	-69.9748	---	0.7836	2.5853	0.7808	1.8011	0.7800
IHA0L03 4:54	-3.3984	-93.2997	---	0.8980	3.1081	0.8622	2.8122	0.8641

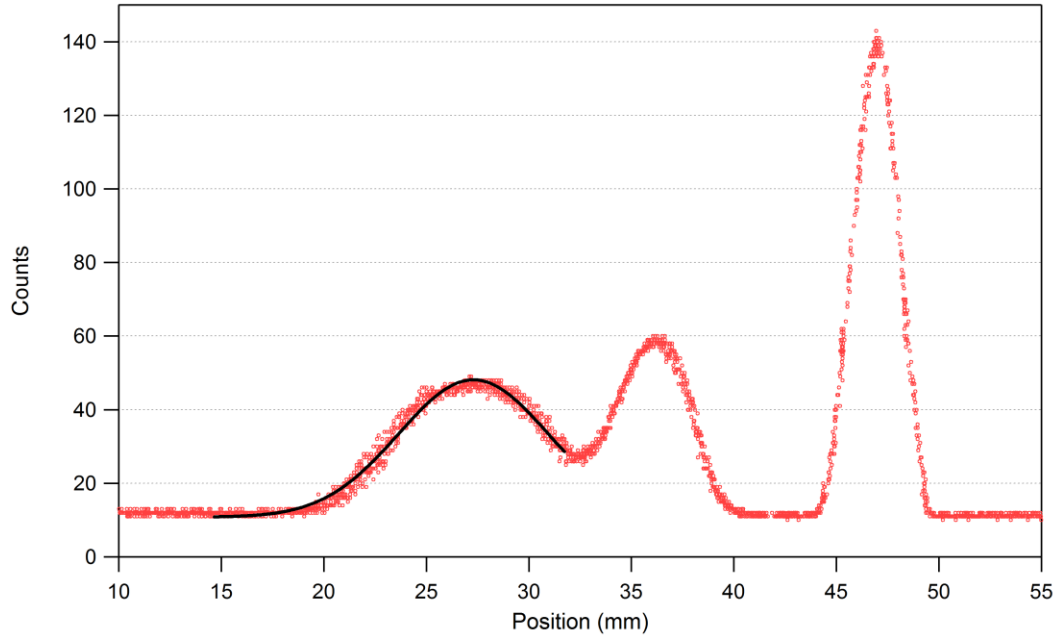


Figure A1: Example fit of the horizontal profile when merged with adjacent peak. Though the fit looks reasonably good, adding the data point to the analysis skews the results (i.e. Twiss parameters).